Structures, Reactivity, and Catalytic Activity of Dithiolato-Bridged Heterobimetallic MRh (M = Pt, Pd) Complexes

Jorge Forniés-Cámer, Anna M. Masdeu-Bultó,* and Carmen Claver

Departament de Química Física i Inorgànica, Universitat Rovira i Virgili, Pl. Imperial Tàrraco 1, 43005 Tarragona, Spain

Cristina Tejel* and Miguel Angel Ciriano

Departamento de Química Inorgánica, Instituto de Ciencia de Materiales de Aragón, Universidad de Zaragoza-CSIC, E-50009 Zaragoza, Spain

Christine J. Cardin

Department of Chemistry, The University of Reading, Whiteknights, P.O. Box 224, Reading RG6 6AD, United Kingdom

Received January 22, 2002

Downloaded by CARLI CONSORTIUM on June 29, 2009
Published on May 22, 2002 on http://pubs.acs.org | doi: 10.1021/om020042r

Heterobimetallic complexes $[(P-P)Pt(\mu\text{-}S-S)Rh(cod)]ClO_4$ (P−P = $(PPh_3)_2$, $Ph_2P(CH_2)_3PPh_2$ (dppp), and $Ph_2P(CH_2)_4PPh_2$ (dppb); S−S = $^-S(CH_2)_2S^-$ (EDT), $^-S(CH_2)_3S^-$ (PDT), $^-S(CH_2)_4S^-$ (BDT), cod = 1,5-cyclooctadiene) reacted with CO to form the carbonyl complexes $[(P-P)Pt(\mu\text{-}S-S)Rh(CO)_2]ClO_4$ and then with PR_3 ligands to give $[(P-P)Pt(\mu\text{-}S-S)Rh(CO)(PR_3)]ClO_4$. The binuclear framework of these cod complexes was maintained in the reactions reported. The cod complexes were tested as catalyst precursors in the hydroformylation of styrene. HPNMR in situ studies showed that mononuclear species formed under catalytic conditions.

Introduction

The interest in heterometallic complexes has been centered on their application as catalyst precursors in homogeneous catalysis processes,[1] as a model for mixed heterogeneous catalysts,[2] and as starting materials for clusters preparation.[3] There are many examples of heterobimetallic complexes with anionic phosphido bridging ligands,[4] or thiolato bridging ligands (RS^-).[4a,5] In contrast, dithiolato ($^-SRS^-$)[6]-bridged heterobimetallic complexes have been studied considerably less, most of the examples being of the early-late (ELHB) type.

We recently described the preparation of a series of complexes $[(P-P)M(\mu\text{-}S-S)Rh(cod)]ClO_4$ (P−P = $(PPh_3)_2$, $Ph_2P(CH_2)_3PPh_2$ (dppp), and $Ph_2P(CH_2)_4PPh_2$ (dppb); M = Pt, Pd; S−S = $^-S(CH_2)_2S^-$ (EDT), $^-S(CH_2)_3S^-$ (PDT), and $^-S(CH_2)_4S^-$ (BDT); cod = 1,5-cyclooctadiene) by direct reaction of the mononuclear complexes $[M(S-S)(P-P)]$ with $[Rh(cod)_2]ClO_4$.[7] We also showed that this synthetic procedure was very versatile by preparing the

* To whom correspondence should be addressed. (A.M.M.-B.) Fax: +34 977 559563. E-mail: masdeu@quimica.urv.es. (C.T.) Fax: +34 976 761187. E-mail: ctejel@posta.unizar.es.

(1) (a) Braunstein, P.; Rose, J. In *Comprehensive Organometallic Chemistry II*; Wilkinson, G., Stone, F. G. A., Abel, E. W., Eds.; Pergamon: Oxford, 1995; Vol. 10, p 351. (b) Farrugia, L. J. *Adv. Organomet. Chem.* **1990**, *31*, 301. (c) The Chemistry of Heteronuclear Clusters and Multimetallic Catalysts; Adams, R. D., Herrmann, W. A., Eds.; *Polyhedron* **1988**, *7*, 2251. (d) Wheatley, N.; Kalck, P. *Chem. Rev.* **1999**, *99*, 3379.

(2) (a) Guczi, L. In *Metal Clusters in Catalysis*; Gates, B. C., Guczi, L., Knozinger, H., Eds.; Elsevier: New York, 1986. (b) Sinfelt, J. H. In *Bimetallic Catalysts: Discoveries, Concepts and Applications;* Wiley: New York, 1983. (c) Xiao, J.; Puddephat, R. J. *Coord. Chem. Rev.* **1995**, *143*, 457. (d) Sachter, W. M. H.; *J. Mol. Catal.* **1984**, *25*, 1. (e) Sinfelt, J. H. *Acc. Chem. Res.* **1977**, *10*, 15. (f) Guczi, L. *J. Mol. Catal.* **1984**, *25*, 13.

(3) Adams, R. D.; Chetcuti, M. J. In *Comprehensive Organometallic Chemistry II;* Wilkinson, G., Stone, F. G. A., Abel, E. W., Eds.; Pergamon: Oxford, 1995; Vol. 10, p 1, p 23.

(4) (a) Stephan, D. W. *Coord. Chem. Rev.* **1989**, *95*, 41. (b) Forniés, J.; Fortuño, C.; Navarro, R.; Martínez, F. *J. Organomet. Chem.* **1990**, *394*, 643. (c) Falvello, L. R.; Forniés, J.; Fortuño, C.; Martínez, F. *Inorg. Chem.* **1994**, *33*, 6242. (d) Braunstein, P.; de Jesús, E.; Dedieu, A.; Lanfranchi, M.; Tiripicchio, A. *Inorg. Chem.* **1992**, *31*, 399. (e) Braunstein, P.; Knorr, M.; Hirle, B.; Reinhard, G.; Schubert, U. *Angew. Chem., Int. Ed. Engl.* **1992**, *31*, 1583. (f) Shyn, S. G.; Lin, P. J.; Dong, T. Y.; Wen, Y. S. *J. Organomet. Chem.* **1993**, *460*, 229. (g) Shyn, S. G.; Lin, P. J.; Wen, Y. S. *J. Organomet. Chem.* **1993**, *443*, 115. (h) Shyn, S. G.; Hsiao, S. M.; Lin, K. J.; Gau, H.-M. *Organometallics* **1995**, *14*, 4300. (i) Shyn, S. G.; Lin, P. J.; Lin, K. J.; Chang, M. C.; Wen, Y. S. *Organometallics* **1995**, *14*, 2253. (j) Shyn, S. G.; Hsu, J. Y.; Lin, P. J.; Wu, W. J.; Peng, S. M.; Lea, G. H.; Wen, Y. S. *Organometallics* **1994**, *13*, 1699. (k) Hsiao, S. M.; Shyn, S. G. *Organometallics* **1998**, *17*, 1151. (l) Oudet, P.; Kubicki, M. M.; Moise, C. *Organometallics* **1994**, *13*, 4278. (m) Boni, G.; Lauvageot, P.; Marpeaux, E.; Moise, C. *Organometallics* **1995**, *14*, 5652. (n) Brettcher, H.-C.; Graf, M.; Merzweiler, K. *J. Organomet. Chem.* **1996**, *525*, 191. (o) Senff, U.; Kurz, S.; Hey-Hawkins, E. *Z. Anorg. Allg. Chem.* **1997**, *623*, 1255.

(5) (a) Jain, V. K. *Inorg. Chim. Acta* **1987**, *133*, 261. (b) White, G. S.; Stephan, D. W. *Organometallics* **1987**, *6*, 2169. (c) Rousseau, R.; Stephan, D. W. *Organometallics* **1991**, *10*, 3399. (d) Capdevila, M.; Gonzalez-Duarte, P.; Foces-Foces, C.; Hernández Cano, F.; Martínez-Ripoll, M. *J. Chem. Soc., Dalton Trans.* **1990**, 143. (e) Darensbourg, M. Y.; Pala, M.; Houliston, S. A.; Kidwell, K. P.; Spencer, D.; Chojnacki, S. S.; Reibenspies, J. H. *Inorg. Chem.* **1992**, *31*, 1487. (f) Amador, U.; Delgado, E.; Forniés, J.; Hernández, E.; Lalinde, E.; Moreno, M. T. *Inorg. Chem.* **1995**, *34*, 5279. (g) Sanchez, G.; Casabó, J.; Molins, E.; Miravitlles, C. *Eur. J. Inorg. Chem.* **1998**, *8*, 1199. (h) Nakahara N.; Hirano, M.; Fukuoka, A.; Komiya, S. *J. Organomet. Chem.* **1999**, *572*, 81.

(6) (a) Aggarwal, R. C.; Mitra, R. *Ind. J. Chem. A* **1994**, *33*, 55. (b) Nadasdi, T. T.; Stephan, D. W. *Inorg. Chem.* **1994**, *33*, 1532. (c) Singh, N.; Prasad, L. B. *Ind. J. Chem. A* **1998**, *37*, 169.

(7) Forniés-Cámer, J.; Masdeu-Bultó, A. M.; Claver, C.; Cardin, C. J. *Inorg. Chem.* **1998**, *37*, 2626.

10.1021/om020042r CCC: $22.00 © 2002 American Chemical Society
Publication on Web 05/22/2002

analogous PtIr complexes [(P−P)Ir(μ-S−S)Rh(cod)]BF_4.[8] Comparison of the crystal structures of the complexes [$(PPh_3)_2$Pt(μ-S−S)Rh(cod)]ClO_4 (S−S = EDT, PDB, BDT), [(dppb)Pt(μ-BDT)Rh(cod)]ClO_4, [(dppp)Pt(μ-BDT)Rh(cod)]ClO_4, and [(dppb)Pd(μ-BDT)Rh(cod)]ClO_4 showed that simple modifications to the alkyl chain of the dithiolate moiety or the use of different phosphines and diphosphines directly affects geometric parameters such as metal−metal distances and angles between coordination planes.

In this paper, we study the reactivity and catalytic activity in the hydroformylation reaction of these complexes. The two main aspects we consider are how structural differences affect the reactivity and how strong the heterobimetallic framework is when exposed to different donor ligands. Thus, we explored the reaction with carbon monoxide and different phosphine and phosphite ligands at normal pressure and under catalytic conditions. We also used cyclic voltammetry to study the redox behavior of these complexes.

Downloaded by CARLI CONSORTIUM on June 29, 2009
Published on May 22, 2002 on http://pubs.acs.org | doi: 10.1021/om020042r

Experimental Section

General Methods. All rhodium complexes were synthesized using standard Schlenk techniques under a nitrogen atmosphere. Solvents were distilled and deoxygenated before use. The complex [$Rh(cod)_2$]ClO_4[9] and diene complexes **1a**−**i**[7] were prepared using methods described in the literature. All other reagents were used as commercially supplied. Elemental analyses were performed on a Carlo-Erba microanalyzer. The IR spectra were obtained using a Nicolet 5ZDX-FT spectrophotometer. ^{1}H NMR spectra were recorded on a Varian Gemini 300 MHz spectrophotometer, and chemical shifts are quoted in ppm downfield from internal $SiMe_4$. FAB mass spectrometry was performed on a VG Autospect in a nitrobenzyl alcohol matrix. Catalytic experiments were performed as previously described.[10] Gas chromatography analyses were performed in a Hewlet-Packard Model 5890 gas chromatograph with flame ionization detector using a 25 m × 0.2 mm Ø capillary column (Ultra 2).

Cyclic voltammetry experiments were performed with an EG&G PARC model 273 potentiostat/galvanostat. The three-electrode glass cell that we used consisted of a platinum-disk working electrode, a platinum-wire auxiliary electrode, and a standard calomel reference electrode (SCE). Tetra-*n*-butylammonium hexafluorophosphate (TBAH) was used as supporting electrolyte. Electrochemical experiments were carried out under nitrogen in ∼5 × 10^{-4} M dichloromethane or MeCN solutions of the complexes and 0.1 M in TBAH. The [$Fe(C_5H_5)_2$]$^+$/[$Fe(C_5H_5)_2$] couple was observed at + 0.47 V under these experimental conditions.

Preparation of Carbonyl Complexes [(P−P)Pt(μ-S−S)Rh(CO)$_2$]ClO_4 (S−S = EDT, PDT, BDT; (P−P) = (PPh_3)$_2$, dppp, and dppb). General Procedure. Carbon monoxide was bubbled for 10 min through dichloromethane solutions of complexes **1a**−**g** (0.05 mmol in ca. 5 mL of solvent). The resulting solution was concentrated to ca. 2 mL. The solid formed by adding hexane was filtered, washed with hexane, and vacuum-dried.

[(PPh_3)$_2$Pt(μ-EDT)Rh(CO)$_2$]ClO_4 (2a): purple crystals (68% yield). ^{1}H NMR (300 MHz, $CDCl_3$, 20 °C): δ 3.32 (m, 2 H, $-CH_2-$, EDT), 2.50 (m, 2 H, $-CH_2-$, EDT), 7.2−7.5 (m, 30 H, Ph, PPh_3). Anal. Calcd for $PtRhClS_2P_2O_6C_{40}H_{34}$: C, 44.88; H, 3.18; S, 5.98. Found: C, 44.56; H, 3.20; S, 5.97. FAB: *m*/*z* 970 [M − ClO_4]$^+$, 914 [M − (CO)$_2$ − ClO_4]$^+$.

[(PPh_3)$_2$Pt(μ-PDT)Rh(CO)$_2$]ClO_4·1/2CH_2Cl_2 (2b): yellow (63% yield). ^{1}H NMR (300 MHz, $CDCl_3$, 20 °C): δ 2.95 (m, 2 H, $-SCH_2-$, PDT), 2.65 (m, 2 H, $-SCH_2-$, PDT), 1.90 (m, 2 H, $-CH_2-$, PDT), 7.3−7.4 (m, 30 H, Ph, PPh_3). Anal. Calcd for $PtRhClS_2P_2O_6C_{41}H_{36}$·1/2$CH_2$ Cl_2: C, 44.22; H, 3.28; S, 5.68. Found: C, 44.13; H, 3.28; S, 5.70. FAB: *m*/*z* 984 [M − ClO_4]$^+$, 928 [M − (CO)$_2$ − ClO_4]$^+$.

[(PPh_3)$_2$Pt(μ-BDT)Rh(CO)$_2$]ClO_4 (2c): yellow (85% yield). ^{1}H NMR (300 MHz, $CDCl_3$, 20 °C): δ 2.20 (m, 4 H, $-SCH_2-$, BDT), 1.60 (m, 4 H, $-CH_2-$, BDT), 7.2−7.5 (m, 30 H, Ph, PPh_3). Anal. Calcd for $PtRhClS_2P_2O_6C_{42}H_{38}$: C, 45.92; H, 3.46; S, 5.83. Found: C, 45.72; H, 3.44; S, 5.81. FAB: *m*/*z* 998 [M − ClO_4]$^+$, 942 [M − (CO)$_2$ − ClO_4]$^+$.

[(dppp)Pt(μ-EDT)Rh(CO)$_2$]ClO_4·CH_2Cl_2 (2d): red (68% yield). ^{1}H NMR (300 MHz, $CDCl_3$, 20 °C): δ 3.00 (m, 2 H, $-SCH_2-$, EDT), 2.80 (m, 2 H, $-SCH_2-$, EDT), 7.4−7.7 (m, 20 H, Ph, dppp), 2.56 (m, 4 H, $-PCH_2-$, dppp), 1.60 (m, 2 H, $-CH_2-$, dppp). Anal. Calcd for $PtRhClS_2P_2O_6C_{31}H_{30}$·$CH_2Cl_2$: C, 36.83; H, 3.07; S, 6.14. Found: C, 36.96; H, 3.11; S, 6.17. FAB: *m*/*z* 858 [M − ClO_4]$^+$, 802 [M − (CO)$_2$ − ClO_4]$^+$.

[(dppp)Pt(μ-BDT)Rh(CO)$_2$]ClO_4·CH_2Cl_2 (2e): yellow (75% yield). ^{1}H NMR (300 MHz, $CDCl_3$, 20 °C): δ 3.20 (m, 4 H, $-SCH_2-$, BDT), 1.2−2.8 (a, 4 H, $-CH_2-$, BDT), 7.3−7.4 (m, 20 H, Ph, dppp), 1.2−2.8 (a, 4 H, $-PCH_2-$, dppp), 1.2−2.8 (m, 2 H, $-CH_2-$, dppp). Anal. Calcd for $PtRhClS_2P_2O_6C_{33}H_{34}$·$CH_2$-$Cl_2$: C, 38.11; H, 3.36; S, 5.97. Found: C, 37.83; H, 3.15; S, 5.86. FAB: *m*/*z* 886 [M − ClO_4]$^+$, 830 [M − (CO)$_2$ − ClO_4]$^+$.

[(dppb)Pt(μ-EDT)Rh(CO)$_2$]ClO_4·CH_2Cl_2 (2f): red (73% yield). ^{1}H NMR (300 MHz, $CDCl_3$, 20 °C): δ 2.98 (m, 2 H, $-CH_2-$, EDT), 2.50 (m, 2 H, $-CH_2-$, EDT), 7.4−7.8 (m, 20 H, Ph, dppb), 2.87 (m, 4 H, $-PCH_2-$, dppb), 1.90 (m, 4 H, $-CH_2-$, dppb). Anal. Calcd for $PtRhClS_2P_2O_6C_{32}H_{32}$·$CH_2Cl_2$: C, 37.48; H, 3.22; S, 6.06. Found: C, 37.23; H, 3.25; S, 6.10. FAB: *m*/*z* 872 [M − ClO_4]$^+$, 816 [M − (CO)$_2$ − ClO_4]$^+$.

[(dppb)Pt(μ-BDT)Rh(CO)$_2$]ClO_4·CH_2Cl_2 (2g): yellow (76% yield). ^{1}H NMR (300 MHz, $CDCl_3$, 20 °C): δ 3.40 (m, 2 H, $-SCH_2-$, BDT), 2.92 (m, 2 H, $-SCH_2-$, BDT), 2.23 (m, 4 H, $-CH_2-$, BDT), 7.4−7.8 (m, 20 H, Ph, dppb), 2.80 (m, 4 H, $-PCH_2-$, dppb), 1.80 (m, 4 H, $-CH_2-$, dppb). Anal. Calcd for $PtRhClS_2P_2O_6C_{34}H_{36}$·$CH_2Cl_2$: C, 38.73; H, 3.50; S, 5.90. Found: C, 38.60; H, 3.47; S, 6.01. FAB: *m*/*z* 900 [M − ClO_4]$^+$, 844 [M − (CO)$_2$ − ClO_4]$^+$.

Preparation of Complexes [(P−P)Pt(μ-S−S)Rh(CO)(PR_3)]ClO_4 (S−S = EDT, PDT, BDT; (P−P) = (PPh_3)$_2$, dppp, and dppb; PR_3 = PPh_3, PCy_3, P(O^{t}BuPh)$_3$). General Procedure. Carbon monoxide was bubbled for 10 min through a dichloromethane solution of the corresponding diolefin complexes **1a**−**g** (0.05 mmol in 5 mL of solvent) to form the corresponding carbonyl complex. The corresponding PR_3 ligand (0.10 mmol) was added, and the solution was stirred for 10 min. The solution was concentrated to 2 mL, and hexane was added to crystallize the products. The solid was filtered, washed with hexane, and vacuum-dried.

[(PPh_3)$_2$Pt(μ-EDT)Rh(CO)(PPh_3)]ClO_4·1/2CH_2Cl_2 (3a): yellow solid (65% yield). ^{1}H NMR (300 MHz, $CDCl_3$, 20 °C): δ 3.19 (m, 1 H, $-CH_2-$, EDT), 3.08 (m, 1 H, $-CH_2-$, EDT), 2.75 (m, 1 H, $-CH_2-$, EDT), 2.25 (m, 1 H, $-CH_2-$, EDT), 7.1−7.5 (m, 45 H, Ph, PPh_3). IR (KBr, cm^{-1}): ν(CO), 1992 (vs). Anal. Calcd for $PtRhClS_2P_3O_5C_{57}H_{49}$·1/2$CH_2Cl_2$: C, 51.26; H, 3.64; S, 4.75. Found: C, 51.25; H, 3.73; S, 4.68. FAB: *m*/*z* 1205 [MH − ClO_4]$^+$, 914 [M − (CO) − PPh_3 − ClO_4]$^+$.

[(PPh_3)$_2$Pt(μ-PDT)Rh(CO)(PPh_3)]ClO_4·1/2CH_2Cl_2 (3b): yellow solid (60% yield). ^{1}H NMR (300 MHz, $CDCl_3$, 20 °C): δ 2.60 (m, 2 H, $-SCH_2-$, PDT), 2.43 (m, 2 H, $-SCH_2-$, PDT), 2.00 (m, 1 H, $-CH_2-$, PDT), 1.84 (m, 1 H, $-CH_2-$, PDT), 7.2−7.6 (m, 45 H, Ph, PPh_3). IR (KBr, cm^{-1}): ν(CO), 1961 (vs). Anal. Calcd for $PtRhClS_2P_3O_5C_{58}H_{51}$·1/2$CH_2Cl_2$: C, 51.62; H, 3.82; S, 4.70. Found: C, 51.33; H, 3.81; S, 4.78. FAB: *m*/*z* 1219 [MH − ClO_4]$^+$.

(8) Forniés-Cámer, J.; Masdeu-Bultó, A. M.; Claver, C. *Inorg. Chem. Commun.* **1999**, *2/3*, 89.
(9) Usón, R.; Oro, L. A.; Ibáñez, F. *Rev. Acad. Cienc. Zaragoza* **1975**, 169.
(10) Masdeu, A. M.; Orejón, A.; Ruiz, A.; Castillón, S.; Claver, C. *J. Mol. Catal.* **1994**, *94*, 149.

Downloaded by CARLI CONSORTIUM on June 29, 2009
Published on May 22, 2002 on http://pubs.acs.org | doi: 10.1021/om020042r

[(PPh$_3$)$_2$Pt(μ-BDT)Rh(CO)(PPh$_3$)]ClO$_4$ (3c): yellow solid (83% yield). ^{1}H NMR (300 Hz, $CDCl_3$, 20 °C): δ 2.40 (m, 1 H, −SCH$_2$−, BDT), 2.18 (m, 3 H, −SCH$_2$−, BDT), 1.98 (m, 2 H, −CH$_2$−, BDT), 1.38 (m, 1 H, −CH$_2$−, BDT), 1.17 (m, 1 H, −CH$_2$−, BDT), 7.1−7.6 (m, 45 H, Ph, PPh$_3$). IR (KBr, cm^{-1}): ν(CO), 1979 (vs). Anal. Calcd for $PtRhClS_2P_3O_5C_{59}H_{53}$: C, 51.52; H, 3.93; S, 4.65. Found: C, 51.39; H, 3.87; S, 4.64. FAB: *m/z* 1233 [MH − ClO_4]$^+$.

[(dppp)Pt(μ-EDT)Rh(CO)(PPh$_3$)]ClO$_4$·1/2CH$_2$Cl$_2$ (3d): yellow solid (72% yield). ^{1}H NMR (300 MHz, $CDCl_3$, 20 °C): δ 3.00 (m, 1 H, −SCH$_2$−, EDT), 2.85 (m, 1 H, −SCH$_2$−, EDT), 2.38 (m, 1 H, −SCH$_2$−, EDT), 2.15 (m, 1 H, −SCH$_2$−, EDT), 6.8−7.8 (m, 35 H, Ph, dppp, PPh$_3$), 2.7−2.8 (m, 4 H, −PCH$_2$−, dppp), 2.10 (m, 2 H, −CH$_2$−, dppp). IR (KBr, cm^{-1}): ν(CO), 1980 (vs). Anal. Calcd for $PtRhClS_2P_3O_5C_{48}H_{45}$·1/2$CH_2Cl_2$: C, 47.16; H, 3.72; S, 5.18. Found: C, 46.98; H, 3.69; S, 5.16. FAB: *m/z* 1092 [M − ClO_4]$^+$.

[(dppp)Pt(μ-BDT)Rh(CO)(PPh$_3$)]ClO$_4$·1/2CH$_2$Cl$_2$ (3e): yellow solid (84% yield). ^{1}H NMR (300 MHz, $CDCl_3$, 20 °C): δ 2.6−3.2 (a, 4 H, −SCH$_2$−, BDT), 1.80 (m, 2 H, −CH$_2$−, BDT), 1.65 (m, 2 H, −CH$_2$−, BDT), 7.2−8.1 (m, 35 H, Ph, dppp, PPh$_3$), 2.45 (m, 4 H, −PCH$_2$−, dppp), 2.00 (m, 2 H, −CH$_2$−, dppp). IR (KBr, cm^{-1}): ν(CO), 1988 (vs). Anal. Calcd for $PtRhClS_2P_3O_5C_{50}H_{49}$·1/2$CH_2Cl_2$: C, 48.02; H, 3.88; S, 5.07. Found: C, 47.92; H, 3.86; S, 4.82. FAB: *m/z* 1120 [M − ClO_4]$^+$.

[(dppb)Pt(μ-EDT)Rh(CO)(PPh$_3$)]ClO$_4$·1/2CH$_2$Cl$_2$ (3f): yellow solid (68% yield). ^{1}H NMR (300 MHz, $CDCl_3$, 20 °C): δ 2.5−3.0 (m, 2 H, −CH$_2$−, EDT), 1.6−2.0 (m, 2 H, −CH$_2$−, EDT), 7.0−7.8 (m, 35 H, Ph, dppb, PPh$_3$), 2.5−3.0 (m, 4 H, −PCH$_2$−, dppb), 1.9−2.3 (m, 4 H, −CH$_2$−, dppb). IR (KBr, cm^{-1}): ν(CO), 1984 (vs). Anal. Calcd for $PtRhClS_2P_3O_5C_{49}H_{47}$·1/2$CH_2Cl_2$: C, 47.59; H, 3.84; S, 5.07. Found: C, 47.71; H, 3.83; S, 5.11. FAB: *m/z* 1106 [M − ClO_4]$^+$.

[(dppb)Pt(μ-BDT)Rh(CO)(PPh$_3$)]ClO$_4$·1/2CH$_2$Cl$_2$ (3g): yellow solid (70% yield). ^{1}H NMR (300 MHz, $CDCl_3$, 20 °C): δ 3.30 (m, 1 H, −SCH$_2$−, BDT), 3.12 (m, 1 H, −SCH$_2$−, BDT), 2.80 (m, 1 H, −SCH$_2$−, BDT), 2.38 (m, 1 H, −SCH$_2$−, BDT), 1.90 (m, 1 H, −CH$_2$−, BDT), 1.60 (m, 1 H, −CH$_2$−, BDT), 1.37 (m, 1 H, −CH$_2$−, BDT), 1.10 (m, 1 H, −CH$_2$−, BDT), 7.2−8.3 (m, 35 H, Ph, dppb and PPh$_3$), 2.80 (m, 4 H, −PCH$_2$−, dppb), 1.70 (m, 4 H, −CH$_2$−, dppb). IR (KBr, cm^{-1}): ν(CO), 1982 (vs). Anal. Calcd for $PtRhClS_2P_3O_5C_{51}H_{51}$·1/2$CH_2Cl_2$: C, 48.43; H, 4.07; S, 5.01. Found: C, 48.63; H, 4.10; S, 4.93. FAB: *m/z* 1134 [M − ClO_4]$^+$.

[(PPh$_3$)$_2$Pt(μ-EDT)Rh(CO)(PCy$_3$)]ClO$_4$·1/2CH$_2$Cl$_2$ (3h): yellow solid (79% yield). ^{1}H NMR (300 MHz, $CDCl_3$, 20 °C): δ 3.35 (m, 2 H, −CH$_2$−, EDT), 2.88 (m, 1 H, −CH$_2$−, EDT), 2.51 (m, 1 H, −CH$_2$−, EDT), 7.2−7.6 (m, 30 H, Ph, PPh$_3$), 1.1−1.9 (m, 33 H, −CH$_2$−, PCy$_3$). IR (KBr, cm^{-1}): ν(CO), 1966 (vs). Anal. Calcd for $PtRhClS_2P_3O_5C_{57}H_{67}$·1/2$CH_2Cl_2$: C, 50.58; H, 4.98; S, 4.69. Found: C, 50.48; H, 5.01; S, 4.09.FAB: *m/z* 1223 [MH − ClO_4]$^+$.

[(PPh$_3$)$_2$Pt(μ-EDT)Rh(CO)(P(O^{t}BuPh)$_3$)]ClO$_4$·1/2CH$_2$Cl$_2$ (3i): yellow solid (88% yield). ^{1}H NMR (300 MHz, $CDCl_3$, 20 °C): δ 3.40 (m, 2 H, −CH$_2$−, EDT), 2.97 (m, 1 H, −CH$_2$−, EDT), 2.51 (m, 1 H, −CH$_2$−, EDT), 6.8−7.7 (m, 42 H, Ph, PPh$_3$, and P(O^{t}BuPh)$_3$), 1.30 (s, 27 H, −CH$_3$, P(O^{t}BuPh)$_3$). IR (KBr, cm^{-1}): ν(CO), 2016 (vs). Anal. Calcd for $PtRhClS_2P_3O_8C_{69}H_{73}$·1/2$CH_2Cl_2$: C, 53.39; H, 4.73; S, 4.09. Found: C, 53.12; H, 4.75; S, 4.12. FAB: *m/z* 1421 [MH − ClO_4]$^+$, 915 [MH − (CO) − P(O^{t}BuPh)$_3$ − ClO_4]$^+$.

Preparation of Complex [(PPh$_3$)$_2$Pt(μ-EDT)Rh(P(OPh)$_3$)$_2$]ClO$_4$·1/2CH$_2$Cl$_2$ (4). Carbon monoxide was bubbled for 10 min through a dichloromethane solution of the corresponding diene complex **1a** (0.05 mmol in 5 mL of solvent) to form the corresponding carbonyl complex. Then, P(OPh)$_3$ (0.10 mmol) was added and the solution was stirred for 10 min. The solution was concentrated to 2 mL, and hexane was added to give a yellow precipitate (79% yield). The solid was filtered, washed with hexane, and vacuum-dried. ^{1}H NMR (300 MHz, $CDCl_3$, 20 °C): δ 2.68 (m, 2 H, −CH$_2$−, EDT), 1.40 (m, 2 H, −CH$_2$−, EDT), 6.8−7.4 (m, 60 H, Ph, PPh$_3$, and P(OPh)$_3$). Anal. Calcd for $PtRhClS_2P_4O_{10}C_{74}H_{64}$·1/2$CH_2Cl_2$: C, 53.34; H, 3.87; S, 3.81. Found: C, 53.09; H, 3.87; S, 3.77. FAB: *m/z* 1535 [MH − ClO_4]$^+$, 914 [M − 2P(OPh)$_3$ − ClO_4]$^+$.

Crystal Data for Complexes [(PPh$_3$)$_2$Pt(μ-EDT)Rh(CO)$_2$]BF$_4$ (2a′) and 3a. Suitable crystals of complexes **2a′** and **3a** were grown by diffusing *n*-hexane into a solution of the complex in dichloromethane and mounted on a glass fiber. The data were collected and processed at room temperature on a Mar Research image plate scanner. Graphite-monochromated Mo Kα radiation was used to measure 95/2 frames, 180 s per frame in both cases.

Compound 2a′: $PtRhS_2P_2O_2C_{40}H_{34}BF_4$·1/2$CH_2Cl_2$, *M* = 1098.9, monoclinic, *a* = 18.407 Å, α = 90°, *b* = 14.162 Å, β = 100.56°, *c* = 32.693 Å, γ = 90°, *V* = 8378.2 Å^3, space group *P*21/*c* (14), *Z* = 4, D_c = 1.743 Mg/m^3, *F*(000) = 4288, purple, crystal dimensions 0.22 × 0.15 × 0.18 mm, μ(Mo Kα) = 19.85 cm^{-1}.

Compound 3a: $PtRhClS_2P_3O_6C_{57}H_{49}$·$CH_2Cl_2$, *M* = 1403.35, triclinic, *a* = 14.246 Å, α = 81.75°, *b* = 14.439 Å, β = 81.06°, *c* = 14.519 Å, γ = 83.15°, *V* = 2905.4 Å^3, space group $P\bar{1}$, *Z* = 2, D_c = 1.604 Mg/m^3, *F*(000) = 1392, yellow, crystal dimensions 0.12 × 0.23 × 0.15 mm, μ(Mo Kα) = 14.67 cm^{-1}.

The XDS[11] package was used to give the following: 7664 unique reflections [merging *R* = 0.0266] (**2a′**) and 5710 unique reflections [merging *R* = 0.0317] (**3a**). The heavy atoms were found from the Patterson map using the SHELX86[12] program and refined subsequently from successive difference Fourier maps using SHELXL93[13] by full-matrix least squares of 528 (**2a′**) and 713 (**3a**) variables, to a final *R*-factor of 0.0619 (**2a′**) and 0.0428 (**3a**) for 7659 (**2a′**) and 5705 (**3a**) reflections with $[F_o] > 4\sigma(F_o)$. All atoms were revealed by the Fourier map difference. Non-hydrogen atoms were refined anisotropically. Hydrogen atoms were placed geometrically and then refined with fixed isotropic atomic displacement parameters. The weighting scheme $w = 1/[\sigma^2(F_o^2) + (aP)^2 + bP]$, where $P = \max((F_o^2, 0) + 2F_c^2)/3$, *a* = 0.0846 (**2a′**), 0.0523 (**3a**) and *b* = 115.82 (**2a′**), 20.68 (**3a**) with $\sigma(F_o)$ from counting statistics, gave satisfactory agreement analyses. The final parameters R_1 ($[F_o] > 4\sigma(F_o)$) were 0.0619 (**2a′**) and 0.0428 (**3a**), and wR_2 (all data) were 0.0777 (**2a′**) and 0.0590 (**3a**) for $R_1 = \sum||F_o| - |F_c||/\sum|F_o|$ and $wR_2 = [\sum w(F_o^2 - F_c^2)/\sum w(F_o^2)^2)]^{1/2}$. The ORTEP diagrams for **2a′** and **3a** were generated using ORTEP-3.[14]

Results and Discussion

***cis*-Dicarbonyl Complexes.** The reaction of the diolefin complexes [(P−P)Pt(μ-S−S)Rh(cod)]ClO_4 (**1a**−**g**) (P−P = (PPh$_3$)$_2$, Ph$_2$P(CH$_2$)$_3$PPh$_2$ (dppp), and Ph$_2$P-(CH$_2$)$_4$PPh$_2$ (dppb); S−S = $^-$S(CH$_2$)$_2$S$^-$ (EDT), $^-$S(CH$_2$)$_3$S$^-$ (PDT), $^-$S(CH$_2$)$_4$S$^-$ (BDT), cod = 1,5-cyclooctadiene, Scheme 1) with carbon monoxide under atmospheric pressure yielded the dicarbonyl complexes [(P−P)Pt(μ-S−S)Rh(CO)$_2$]ClO_4 (**2a**−**g**, Scheme 1), which were isolated in good yields.

The dinuclear framework was maintained in these reactions as deduced from the spectroscopic data, which confirmed the proposed formulations and revealed the lack of bridge cleavage and ligand redistribution processes. The *m/z* peaks of the cations were observed in the FAB+ mass spectra, while the IR spectra showed two ν(CO) bands separated by ca. 60 cm^{-1} as expected

(11) Kabsch, W. J. *Appl. Crystallogr.* **1993**, *26*, 795.
(12) Sheldrick, G. M. *SHELXS-86*: Program for Crystal Structure Solutions; University of Göttingen: Germany, 1986.
(13) Sheldrick, G. M. *SHELXS-93*: Program for Crystal Structure Solutions; University of Göttingen: Germany, 1993.
(14) Farrugia, L. J. *ORTEP-3 for Windows. J. Appl. Crystallogr.* **1997**, *30*, 565.

Table 1. Infrared (cm^{-1})[a] and $^{31}P\{^1H\}$ NMR[b] (δ) Data for Complexes 2a−g

complex	ν(CO)	$\delta(^{31}P)$	$^1J_{Pt-P}$ (Hz)
$[(PPh_3)_2Pt(\mu\text{-EDT})Rh(CO)_2]ClO_4$ (**2a**)	2075 vs, 2023 vs	14.73	3265
$[(PPh_3)_2Pt(\mu\text{-PDT})Rh(CO)_2]ClO_4$ (**2b**)	2089 vs, 2012 vs	17.32	3155
$[(PPh_3)_2Pt(\mu\text{-BDT})Rh(CO)_2]ClO_4$ (**2c**)	2076 vs, 2018 vs	18.51	2955
$[(dppp)Pt(\mu\text{-EDT})Rh(CO)_2]ClO_4$ (**2d**)	2060 vs, 2011 vs	−2.89	3004
$[(dppp)Pt(\mu\text{-BDT})Rh(CO)_2]ClO_4$ (**2e**)	2088 vs, 2024 vs	0.01	2765
$[(dppb)Pt(\mu\text{-EDT})Rh(CO)_2]ClO_4$ (**2f**)	2064 vs, 2015 vs	14.03	3142
$[(dppb)Pt(\mu\text{-BDT})Rh(CO)_2]ClO_4$ (**2g**)	2087 vs, 2013 vs	17.50	2917

[a] Spectra recorded in CH_2Cl_2. [b] Spectra recorded in $CDCl_3$. Chemical shifts are referenced to H_3PO_4 ($\delta = 0$ ppm). vs = very strong.

Scheme 1

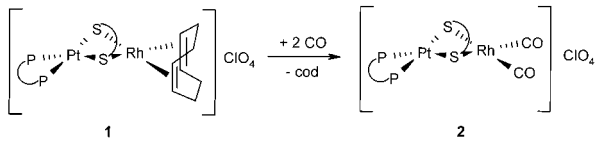

1 2

	P−P	S−S
a	$(PPh_3)_2$	EDT
b	$(PPh_3)_2$	PDT
c	$(PPh_3)_2$	BDT
d	dppp	EDT
e	dppp	BDT
f	dppb	EDT
g	dppb	BDT

for rhodium *cis*-dicarbonyl compounds (Table 1).[15] In addition, the two equivalent phosphorus nuclei bonded to platinum produced a singlet with the corresponding ^{195}Pt satellites in the $^{31}P\{^1H\}$ NMR spectra (Table 1). The P−Pt coupling constants were in the normal range for Pt(II) complexes[16] and slightly larger than those of the corresponding cod complexes (**1a**−**g**). The ^1H NMR spectra of complexes with an EDT ligand (**2a, 2d, 2f**) showed the methylenic protons as two signals in the 2.5−3.5 ppm region, which were identified by $^1H,^1H$−COSY experiments. The signals attributed to the protons oriented toward the platinum center were more deshielded (ca. 3.5 ppm) than those oriented toward rhodium (ca. 2.5 ppm), as previously reported.[7] The complexes with the BDT ligand (**2c**, **2e, 2g**) showed a wide nonresolved signal in this region.

X-ray Structure of the Complex $[(PPh_3)_2Pt(\mu\text{-EDT})Rh(CO)_2]BF_4$ (2a′). Crystals suitable for X-ray analysis of the tetrafluoroborate analogues of complex **2a** (**2a′**) were grown by diffusing *n*-hexane into a solution of the complex in dichloromethane. The binuclear cation $[(PPh_3)_2Pt(\mu\text{-EDT})Rh(CO)_2]^+$ represented in Figure 1 has a bent structure in which the dithiolate is bonded as a bridge ligand to both metal atoms, each of which has a square-planar environment. Selected bond distances and angles are given in Table 2.

The distance Rh−Pt (2.9826(9) Å) is longer than the value considered for the Pt−Rh metal−metal bond (2.6 Å). Nevertheless, it is shorter than the distance for the analogous diene complex $[(PPh_3)_2Pt(\mu\text{-EDT})Rh(cod)]ClO_4$ (3.0096(6) Å)[7] and one of the shortest reported in the literature for nonbonded Rh−Pt atoms.[17]

The intercationic rhodium−rhodium distances found in the packed structure are quite long (4.481 Å) to

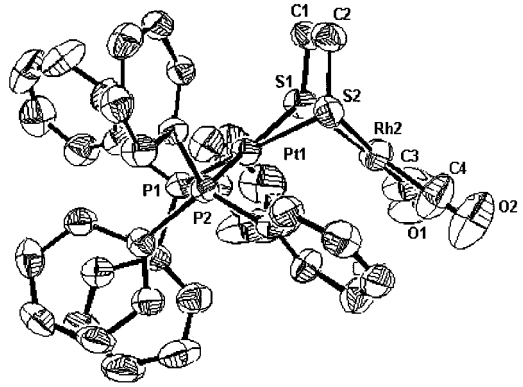

Figure 1. X-ray structure of the cation $[(PPh_3)_2Pt(\mu\text{-EDT})Rh(CO)_2]^+$ of complex **2a′** showing thermal ellipsoids at 50% probability.

Table 2. Selected Bond Lengths (Å) and Angles (deg) for Complex 2a′

Pt(1)−Rh(2)	2.9826(9)	P(2)−Pt(1)−Rh(2)	120.83(7)
Pt(1)−P(1)	2.296(2)	P(1)−Pt(1)−Rh(2)	120.28(6)
Pt(1)−P(2)	2.281(2)	S(1)−Pt(1)−Rh(2)	51.00(7)
Pt(1)−S(1)	2.369(3)	S(2)−Pt(1)−Rh(2)	50.98(6)
Pt(1)−S(2)	2.377(3)	C(3)−Rh(2)−C(4)	90.9(7)
Rh(2)−C(3)	1.856(12)	C(3)−Rh(2)−S(1)	95.7(5)
Rh(2)−C(4)	1.89(2)	C(4)−Rh(2)−S(1)	172.8(4)
Rh(2)−S(1)	2.370(3)	C(3)−Rh(2)−S(2)	173.9(5)
Rh(2)−S(2)	2.370(3)	C(4)−Rh(2)−S(2)	94.8(5)
P(2)−Pt(1)−P(1)	101.34(9)	S(1)−Rh(2)−S(2)	78.51(10)
P(2)−Pt(1)−S(1)	166.06(10)	S(1)−Rh(2)−Pt(1)	50.99(7)
P(1)−Pt(1)−S(1)	92.52(10)	S(2)−Rh(2)−Pt(1)	51.19(6)
P(2)−Pt(1)−S(2)	87.87(9)	Pt(1)−S(1)−Rh(2)	78.01(9)
P(1)−Pt(1)−S(2)	170.27(9)	Rh(2)−S(2)−Pt(1)	77.84(8)
S(1)−Pt(1)−S(2)	78.39(10)	$\Theta(PtS_2Rh)$	108.5
φ	106.4		

propose a weak rhodium−rhodium interaction since the distances reported for complexes with unidirectional packing as a result of intermetallic interactions are somewhat shorter. Some examples are $[Rh(acac)(CO)_2]$, which has a Rh···Rh distance of 3.26 Å,[18] or the dinuclear complex $[Rh(\mu\text{-Cl})(CO)_2]_2$ with a Rh···Rh distance of 3.31 Å.[19]

The metal−ligand bond distances are in the range observed for related heterobimetallic PtRh complexes with dithiolate bridge ligands.[7] The Pt−P bond distances (average 2.288 Å) are similar to the ones for diene complex **1a** (average 2.276 Å) and mononuclear complex

(15) Nakamoto, K. In *Infrared and Raman Spectra of Inorganic and Coordination Compounds*, 5th ed.; Wiley: New York, 1997.
(16) Verkade, V. G.; Quin, L. D. In *Phosphorus-31 NMR Spectroscopy in Stereochemical Analysis Organic Compounds and Metal Complexes*; VCH Publishers: Deerfield, 1987.

(17) (a) Guimerans, R. R.; Wood, F. E.; Balch, A. L. *Inorg. Chem.* **1984**, *23*, 1307. (b) Balch, A. L.; Guimerans, R. R.; Linehan, J.; Wood, F. E. *Inorg. Chem.* **1985**, *24*, 2021. (c) Hutton, A. T.; Langrick, C. R.; McEwan, D. M.; Pringle, P. G.; Shaw, B. L. *J. Chem. Soc., Dalton Trans.* **1985**, 2121. (d) Balch, A. L.; Catalano, V. J. *Inorg. Chem.* **1992**, *31*, 3934.
(18) Bailey, N. A.; Coates, E.; Robertson, G. B.; Bonati, F.; Ugo, R. J. *J. Chem. Soc., Dalton Trans.* **1967**, 1041.
(19) Dahl, L. F.; Martell, C.; Wampler, D. L. *J. Am. Chem. Soc.* **1961**, *83*, 1761.

Downloaded by CARLI CONSORTIUM on June 29, 2009
Published on May 22, 2002 on http://pubs.acs.org | doi: 10.1021/om020042r

Table 3. $^{31}P\{^1H\}$ NMR[a] (δ) Data for Complexes 3a−i and 4

complex	P_a	P_b[b]	P_c[b]	$^1J_{Pa-Rh}$	$^1J_{Pb-Pt}$	$^1J_{Pc-Pt}$	$^4J_{Pa-Pb}$	$^4J_{Pa-Pc}$	$^2J_{Pb-Pc}$	$^3J_{Pb-Rh}$	$^3J_{Pc-Rh}$
3a	36.3	16.2	14.4	156	3240	3104	4.6	8.2	17.9	1.4	1.3
3b	39.1	20.4	16.5	153	3149	2957	4.1	18.0	18.0	1.8	
3c	41.8	20.7	17.8	148	2946	2816	5.6	22.2	14.7	1.4	
3d	36.8	−3.9	−4.9	156	2989	2922	3.3	6.9	29.4		
3e	42.8	0.6	−0.9	146	2708	2707	5.5	20.0	23.8		
3f	36.7	17.3	7.9	157	3165	2970	3.6	7.3	23.0		
3g	43.4	17.8	15.1	148	2838	2853	5.6	19.3	17.4		
3h	51.2	17.3	13.8	150	3226	3070	4.1	6.5	18.5	1.3	1.3
3i	114.7	14.8	13.7	269	3308	3052	6.4	11.4	17.8	1.0	
4	116.9	15.2		284	3119						*a*

[a] Spectra recorded in $CDCl_3$. Chemical shifts are referenced to H_3PO_4 (δ = 0 ppm). [b] Assignation for P_b and P_c may be the opposite.

cis-[Pt(EDT)(PPh_3)$_2$] (average 2.2885 Å).[20] This distance, however, is longer than the one for the dichloro analogue *cis*-[$PtCl_2(PPh_3)_2$] (average 2.258 Å).[21]

The Rh−S distances in complex **2a′** (average 2.370 Å) are longer than in diene complex **1a** (average 2.359 Å), which is attributed to the fact that the *trans* influence of the carbonyl ligand is greater than that of the cod ligand. Pt−S bond distances are also slightly longer in complex **2a′** than in the cod complex.

The torsion angle Θ (RhS_2Pt) of the bent structure of **2a′** (108.5°) is smaller than that of the diene complex **1a** (111.27°). This may be because the steric repulsion between the terminal ligands in the dicarbonylic complex is lower. By comparing **2a′** with the related homobinuclear complexes [Rh_2(μ-EDT)(cod)$_2$] or [Rh_2(μ-PDT)-(cod)$_2$], which have torsion angles of 104°,[22] we can conclude that the triphenylphosphino terminal ligands produce a repulsion that opens the bent structure.

The angle between the coordination planes without the metal atoms (φ) in **2a′** is 106.4°, which is ca. 2° difference with respect to Θ. This small difference between φ and Θ indicates that the metal atom is only slightly separated from the coordination plane. In diene complex **1a** the differences between φ and Θ were greater (111.27° and 96.02°, respectively) and were attributed to intermetallic repulsion due to the short metal−metal distance.[22]

Reactions of Complexes 2a−g with Phosphines, Phosphites, and the Diphosphine dppp. The addition of 1 molar equiv of PPh_3 to the dicarbonyl complexes [(P−P)Pt(μ-S−S)Rh(CO)$_2$]ClO_4 (**2a**−**g**) produced the replacement of one carbonyl group with formation of the complexes [(P−P)Pt(μ-S−S)Rh(CO)(PPh_3)]ClO_4 (**3a**−**g**, Scheme 2). In a similar way, complex **2a** reacted with the bulky PCy_3 and P(O-*o*-^{t}BuPh)$_3$ ligands to give [(PPh_3)$_2$Pt(μ-EDT)Rh(CO)(PR_3)]ClO_4 (R = Cy (**3h**), O-*o*-^{t}BuPh (**3i**)). No reaction was observed between the cod compounds **1a**−**g** and PPh_3. Complexes **3a**−**i** were isolated in good yields, and the IR spectra showed only one absorption in the ν(CO) region, which confirmed their formulation. The ν(CO) frequencies of the EDT complexes with different PR_3 ligands were in the order **3h** < **3a** < **3i**. This was the expected order because of the basicity of the PR_3 ligands PCy_3 > PPh_3 > P(O-*o*-^{t}BuPh)$_3$.

Scheme 2

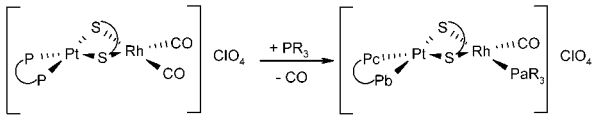

2 3

	P-P	S-S	PR_3
a	(PPh_3)$_2$	EDT	PPh_3
b	(PPh_3)$_2$	PDT	PPh_3
c	(PPh_3)$_2$	BDT	PPh_3
d	dppp	EDT	PPh_3
e	dppp	BDT	PPh_3
f	dppb	EDT	PPh_3
g	dppb	BDT	PPh_3
h	(PPh_3)$_2$	EDT	PCy_3
i	(PPh_3)$_2$	EDT	P(O-*o*-*tert*BuC_6H_4)$_3$

Scheme 3

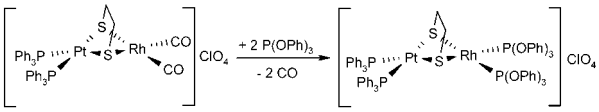

2a 4

The $^{31}P\{^1H\}$ NMR spectra of complexes **3a**−**i** (Table 3) displayed three signals, one of which showed a ^{103}Rh−P coupling (P_a, Scheme 2) and the other two showed the characteristic satellites of a ^{195}Pt−P coupling (P_b and P_c, Scheme 2). The signals corresponding to P_b and P_c were assigned on the basis of the structural data of complex **3a**, assuming that the signal with the largest Pt−P coupling constant is the one with the shortest Pt−P distance. As the shortest Pt−P distance in the X-ray structure of complex **3a** (discussed in the next section) corresponds to the phosphorus *cis* to the Rh−P bond, the signal at δ 16.2 ppm was attributed to P_b and the signal at 14.4 ppm was assigned to P_c.

The reaction between **2a** and 1 molar equiv of the less bulky phosphite, $P(OPh)_3$, produced mixtures of the species [(PPh_3)$_2$Pt(μ-EDT)Rh(CO){$P(OPh_3)$}]ClO_4 and [(PPh_3)$_2$Pt(μ-EDT)Rh{$P(OPh_3)$}$_2$]ClO_4 (**4**), which evolved to **4** when the second molar equivalent of $P(OPh)_3$ was added (Scheme 3). The ^{1}H NMR spectrum of **4** showed two signals corresponding to the two different methylenic environments of the EDT ligand (see Experimental Section). These methylenic signals are shielded considerably more than those of parent complex **2a,** which may be because the π-acceptor ability of the phosphite is less than that of the carbonyl ligand.

Since diphosphines have shown interesting applications in homogeneous catalysis due to their ability to control the selectivity,[23] we studied the reactivity of the carbonyl complexes toward the diphosphine dppp. The

(20) Bryan, S. A.; Roundhill, D. M. *Acta Crystallogr., C: Cryst. Struct. Commun.* **1983**, *39*, 184.
(21) Fergusson, G.; Anderson, G. K.; Clark, H. C.; Davies, J. A.; Parvez, M. *J. Cryst. Spectrosc. Res.* **1982**, *12*, 449.
(22) Masdeu, A..M.; Ruiz, A.; Castillón, S.; Claver, C.; Hitchcock, P. B.; Chaloner, P.; Bo, C.; Poblet, J. M.; Sarasa, P. *J. Chem. Soc., Dalton Trans.* **1993**, 268.

Downloaded by CARLI CONSORTIUM on June 29, 2009
Published on May 22, 2002 on http://pubs.acs.org | doi: 10.1021/om020042r

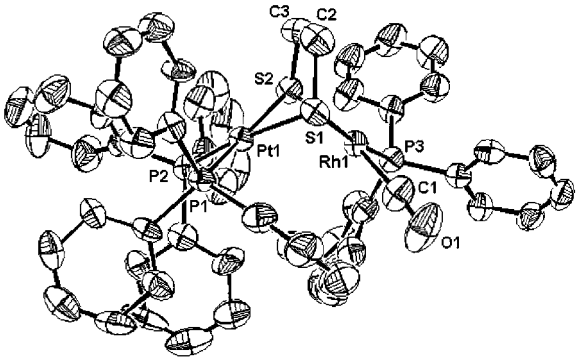

Figure 2. X-ray structure of the cation $[(PPh_3)_2Pt(\mu\text{-EDT})Rh(CO)(PPh_3)]^+$ of complex **3a** showing thermal ellipsoids at 50% probability for the two enantiomers.

$^{31}P\{^1H\}$ NMR spectrum of a solution of **2a** with 2 molar equiv of dppp in $CDCl_3$ indicated that a mixture of complexes formed as a result of a bridge-cleavage reaction. These products were the mononuclear complex $[Pt(EDT)(PPh_3)_2]$, which showed a singlet with Pt−P satellites at 21.0 ppm, as previously described,[24] and the pentacoordinated species $[Rh(dppp)_2(CO)]^+$, which showed broad signals at 15.6 and −10.3 ppm, resolved at −65 °C as two double triplets with $J_{PP} = 45$ Hz, $J_{PaxRh} = 86.3$ Hz, $J_{PeqRh} = 113.6$ Hz,[25] and free ligand. Two small signals at −2 and −4 ppm were also detected.

To sum up, the heterobimetallic cod complexes **1a**−**g** reacted with PR_3 donor ligands in the presence of carbon monoxide and maintained the heterobimetallic structure, while **1a** reacted with the diphosphine dppp in the presence of carbon monoxide and led to the rupture of the dinuclear framework.

X-ray Structure of Complex 3a. The crystal structure of complex **3a** (Figure 2) was determined by X-ray diffraction of a suitable crystal that had been obtained by diffusing *n*-hexane through a solution of the complex in dichloromethane. Complex **3a** is an example of a chiral complex in which none of the ligands are chiral. The X-ray structure was obtained from the racemic sample, so both enantiomers were observed in the unit cell. The structure of the cation complex of **3a** is bent, analogous to the related dithiolate bridge complex **2a′**. Selected bond distances and angles are given in Table 4.

There is no metal−metal bond since the PtRh distance is 3.022(2) Å. The PtRh distance of **3a** is longer than that of **2a′**, presumably because of the steric repulsion between the triphenylphosphine terminal ligands bonded to the different metals.

The Rh−C bond distance (1.836(14) Å) is shorter in complex **3a** than in complex **2a′** (average 1.873 Å), which indicates that there is an increase in the back-bonding nature of the Rh−CO bond. This is because a strong π-acceptor ligand such as CO is replaced by a better donor and less acceptor ligand such as triphenylphosphine. The variation in the bond distances agrees with the variation in the stretching ν(CO) bands in the IR spectrum.

Table 4. Selected Bond Lengths (Å) and Angles (deg) for Complex 3a

Pt(1)−P(2)	2.278(3)	S(1)−Pt(1)−Rh(1)	51.34(6)
Pt(1)−P(1)	2.301(2)	S(2)−Pt(1)−Rh(1)	50.55(7)
Pt(1)−S(1)	2.357(3)	C(1)−Rh(1)−P(3)	89.4(4)
Pt(1)−S(2)	2.362(2)	C(1)−Rh(1)−S(2)	168.6(4)
Pt(1)−Rh(1)	3.0217(8)	P(3)−Rh(1)−S(2)	97.53(9)
Rh(1)−C(1)	1.836(14)	C(1)−Rh(1)−S(1)	96.6(4)
Rh(1)−P(3)	2.275(3)	P(3)−Rh(1)−S(1)	172.00(10)
Rh(1)−S(2)	2.375(3)	S(2)−Rh(1)−S(1)	77.40(9)
Rh(1)−S(1)	2.406(3)	Pt(1)−S(1)−Rh(1)	78.74(8)
C(1)−O(1)	1.138(14)	Pt(1)−S(2)−Rh(1)	79.28(8)
P(2)−Pt(1)−P(1)	99.11(9)	$\Theta(PtS_2Rh)$	109.9
P(2)−Pt(1)−S(1)	169.40(9)	φ	103.7
P(1)−Pt(1)−S(1)	88.66(9)		
P(2)−Pt(1)−S(2)	94.10(9)		
P(1)−Pt(1)−S(2)	166.50(9)		
S(1)−Pt(1)−S(2)	78.61(9)		

The Rh−S(1) bond distance *trans* to the Rh−PPh_3 bond (2.406(3) Å) is longer than the Rh−S(2) distance (2.375(3) Å) *trans* to the carbonyl ligand. This is because the PPh_3 ligand has a greater *trans* influence than the carbonyl ligand.[26] This was also observed in related mixed complexes such as *cis*-$[Ir(\mu\text{-}S^tBu)(CO)(P(OMe)_3)]_2$, where the Ir−S *trans* to $P(OMe)_3$ is 2.393 Å while the distance Ir−S *trans* to CO is 2.386 Å.[27]

The different *trans* influence of PPh_3 and CO is reflected in the Pt−P distances. The longest Pt−P distance is Pt−P(2), which is *trans* to Pt−S(1) and experiences the greater *trans* influence of the PPh_3 ligand. This can be considered a long-range *trans* influence: it acts through two *trans* bonds and finally, because of the binuclear structure of the complex, it is also detected in a position *cis* to the original ligand.

Taking into account that the shorter Pt−P distance should correspond to the greater $^{195}Pt-^{31}P$ coupling, we assigned the P(2) that is *cis* to P(3) to the $^{31}P\{^1H\}$ NMR signal named P_b.

The difference between the angles φ and Θ (109.9° and 103.7°, respectively) is in this case greater than for complex **2a′**. The whole hinge structure is twisted due to the repulsion between the terminal triphenylphosphine ligands. The angles between the ligands are far from the theoretical 90°: in fact they range between 97.53(9)° for P(3)−Rh(1)−S(2) and 77.40(9)° for S(1)−Rh(1)−S(2). The deviation in the planarity can also be observed in the *trans* angles such as C(1)−Rh(1)−S(2) with a value of 168.6(4)° or P(1)−Pt(1)−S(2) with a value of 166.50(9)°.

Cyclic Voltammetry and Chemical Oxidation Studies. We used cyclic voltammetry (CV) to study the electrochemical behavior of some selected complexes. The complexes $[(PPh_3)_2Pt(\mu\text{-}S{-}S)Rh(cod)]$ (S−S = EDT (**1a**), PDT (**1b**), BDT (**1c**)), whose environments are identical at the metal centers, were chosen as the most appropriate ones to show how the dithiolate bridge affects the redox properties of these heterobimetallic complexes. Compounds **1a** and **1c** showed a wave with $(E_p^a + E_p^c)/2$ values of 0.97 and 0.95 V at 0.2 V s^{-1}, respectively. In both cases, the ip_c/ip_a ratio was below 1.00 and decreased as the scan rate was reduced, which is indicative of a coupled irreversible chemical reaction.

(23) Pignolet, L. H. In *Homogeneous Catalysis with Metal Phosphine Complexes*; Plenum Press: New York, 1983.
(24) Rauchfuss, T. B.; Shu, J. S.; Roundhill, D. M. *Inorg. Chem.* **1976**, *15*, 2096.
(25) James, B. R.; Mahajan, D. *Can. J. Chem.* **1980**, *58*, 996.
(26) Appleton, T. G.; Clark, H. C.; Manzer, L. E. *Coord. Chem. Rev.* **1977**, *77*, 313.
(27) Bonnet, J. J.; Thorez, A.; Maisonnat, A.; Galy, J.; Poilblanc, R. *J. Am. Chem. Soc.* **1979**, *101*, 5940.

Downloaded by CARLI CONSORTIUM on June 29, 2009
Published on May 22, 2002 on http://pubs.acs.org | doi: 10.1021/om020042r

Downloaded by CARLI CONSORTIUM on June 29, 2009
Published on May 22, 2002 on http://pubs.acs.org | doi: 10.1021/om020042r

For complex **1b** the oxidation process was irreversible, while the CV showed only the anodic peak at 1.1 (at 0.2 V s^{-1}), and the reverse scan showed no cathodic peak even at scan rates around 1 V s^{-1}. Modifications to the phosphorus ligands at the platinum center produced no significant variation in the $(E_p^a + E_p^c)/2$ values or wave features. Thus, the CVs of the compounds [(P−P)Pt(μ-EDT)Rh(cod)]] (P−P = dppp (**1d**), dppb (**1f**)) were similar to those of **1a** with $(E_p^a + E_p^c)/2$ values of 0.94 V at 0.2 V s^{-1} for both complexes. On the other hand, modifications to the ancillary ligands at the rhodium center produced important differences. The complex $[(PPh_3)_2Pt(\mu\text{-EDT})Rh(CO)_2]$ (**2a**) was found to give no voltammetric wave in the 0−1.4 V region, but the related $[(PPh_3)_2Pt(\mu\text{-EDT})Rh(CO)(PPh_3)]$ (**3a**) showed an irreversible oxidation peak at 1.21 V (at 0.2 V s^{-1}). In addition, the electrogenerated species showed an irreversible reduction wave at 0.70 V (at 0.2 V s^{-1}). These results indicate that the oxidation process of these complexes produces unstable species that undergo further chemical reactions. Moreover, attempts to isolate the oxidation products on a preparative scale led to only mixtures of unidentified compounds. As the oxidation process depends essentially on the chemical environment of the rhodium atoms, electrons are probably removed at this center. However, the dithiolate ligands may undergo associated chemical reactions leading to the formation of dithiolate radicals or disulfides. In fact, the oxidation of thiols with metal ions can easily lead to the formation of disulfides, as is well documented in the literature.[28]

Hydroformylation Studies. The use of homodinuclear rhodium complexes as catalyst precursors in the hydroformylation of alkenes had been extensively studied,[29] although, posterior high-pressure IR studies in situ have shown that mononuclear species are formed under catalytic conditions in the case of monothiolate dinuclear rhodium systems with monophosphines or monophosphites.[30] Nevertheless, for the dithiolate systems no mononuclear species were observed by HPIR under catalytic conditions, although there was indirect evidence of bridge cleavage. To determine whether heterodinuclear complexes would behave differently, we studied the catalytic activity of heterobimetallic PtRh complexes with the dithiolate BDT^{2-} **1c**, **1e**, **1g** for the hydroformylation of styrene (eq 1). The effect of the second metal was studied using the palladium complexes $[(dppp)Pd(\mu\text{-BDT})Rh(cod)]ClO_4$ (**1h**) and $[(dppb)Pd(\mu\text{-BDT})Rh(cod)]ClO_4$ (**1i**) as catalyst precursors. The results obtained with these systems are summarized in Table 5. Hydrogenation of styrene was not observed in any case.

$$Ph{-}CH_2{=}CH_2 + CO + H_2 \xrightarrow{[catal]} Ph{-}CH(CHO){-}CH_3 + Ph{-}CH_2{-}CH_2CHO \quad (1)$$

The reaction conditions optimized for catalyst precursor **1c**, which contains the BDT dithiolate ligand, showed that results were best at 10 atm, 50 °C, and a P/Rh ratio of 4 (96% aldehyde conversion) and 91% of 2-phenylpropanal (entry 1, Table 5). The conversion was very low in the absence of PPh_3 (entry 2, Table 5). Analysis of the samples at consecutive reaction times in experiment 1 showed that the regioselectivity in 2-phenylpropanal evolves slowly from 84% after 1 h reaction (at 1% conversion) to 91% after 24 h.

Table 5. Hydroformylation of Styrene Using the [(P−P)M(μ-BDT)Rh(cod)]ClO_4/P−P Systems (P−P = $(PPh_3)_2$ and M = Pt (1c), dppp and M = Pt (1e), P−P = dppp and M = Pd (1h), P−P = dppb and M = Pt (1g), P−P = dppb and M = Pd (1i)) and $[Rh(cod)_2]ClO_4$ (5) as Catalyst Precursors[a]

entry	prec	% conv[b]	% 2-PP[c]/3-PP[d]
1	**1c**/PPh_3	96	91/9
2	**1c**	2	81/19
3	**5**/PPh_3	96	91/9
4	**1e**/dppp	2	77/23
5	**1h**/dppp	17	93/7
6	**5**/dppp	51	70/30
7	**1g**/dppb	4	96/4
8	**1i**/dppb	56	91/9
9	**5**/dppb	8	83/17

[a] Reaction conditions: styrene (4 mmol), complex (0.01 mmol), tetrahydrofurane (10 mL), P/Rh = 4, pressure = 10 bar, CO/H_2 = 1, T = 50 °C, t = 24 h. [b] Aldehyde conversion measured by chromatography integral ratio. [c] 2-phenylpropanal. [d] 3-phenylpropanal.

To determine whether mononuclear Rh phosphine−carbonyl complexes were responsible for the catalytic activity, the related cationic mononuclear complex $[Rh(cod)_2]ClO_4$ **5** was used as catalyst precursor adding PPh_3 with the same P/Rh ratio (entry 3, Table 5). In this case, the conversion and regioselectivity in 2-phenylpropanal are identical to those observed for the precursor **1c**/PPh_3. Therefore, these results suggest that mononuclear species are formed under reaction conditions in both cases and no particular advantage is observed using the heterobimetallic precursors.

In general, the heterobimetallic−diphosphine catalytic systems showed lower conversions than the PPh_3 systems. Since the final catalytic solutions showed no decomposition, the lower conversions could be attributed to lower catalytic activity. On the other hand, the catalytic behavior observed for the diphosphine platinum (**1e** and **1g**) and palladium (**1h** and **1i**) precursor systems was different, as shown in Table 5 (entries 4−9).

In general, the PdRh−diphosphine systems provide higher conversions at the same reaction times, and the regioselectivities of the reaction were also different depending on the second metal (see for example entry 5 (PdRh) compared to entry 4 (PtRh) in Table 5).

Under the same conditions, the results obtained with the mononuclear species **5** with diphosphines (entries 6 and 9, Table 5) are different from the ones obtained with the heterobimetallic systems.

Although [M(dithiolate)(diphosphine)] (M = Pt, Pd) species may form under catalytic conditions, it is important to note that they do not participate in the catalytic activity since [Pt(dithiolate)(P−P)] (dithiolate = EDT, PDT, and BDT; P−P = $(PPh_3)_2$, dppp, and dppb) complexes are not active unless $SnCl_2$ is not added.[31] Likewise, when [Pd(BDT)(dppb)]/dppb was used as catalyst precursor under the same conditions, no alde-

(28) Uemura, S. In *Comprehensive Organic Synthesis*; Trost, B. M., Fleming, I., Eds.; Pergamon: Oxford: U.K., 1991; Vol. 7, Chapter 6.2.
(29) Bayón, J. C.; Claver, C.; Masdeu-Bultó, A. M. *Coord. Chem. Rev.* **1999**, *193*, 73.
(30) Diéguez, M.; Claver, C.; Masdeu-Bultó, A. M.; Ruiz, A.; van Leeuwen, P. W. N. M.; Schoemaker, G. C. *Organometallics* **1999**, *18*, 2107.

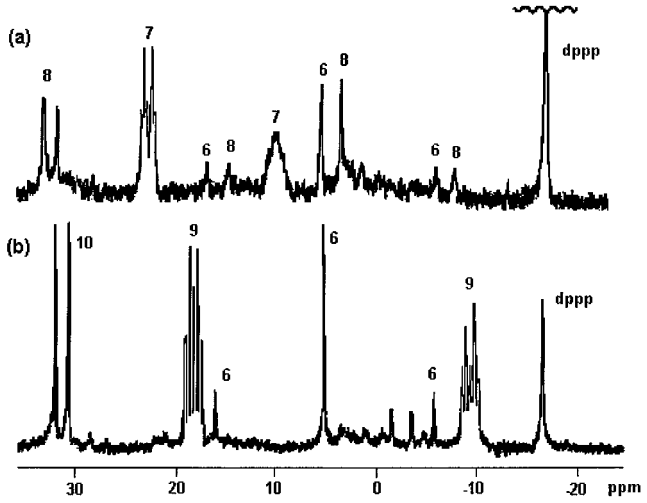

Figure 3. $^{31}P\{^1H\}$ NMR spectrum of **1e**/2dppp in THF: (a) under 5 atm of H_2, (b) under total 10 atm (5 atm of H_2 and 5 atm of CO).

Downloaded by CARLI CONSORTIUM on June 29, 2009
Published on May 22, 2002 on http://pubs.acs.org | doi: 10.1021/om020042r

hydes were detected. Thus, in this case the active center is the rhodium.

In conclusion, the results obtained in the hydroformylation of styrene with heterobimetallic complexes with triphenylphosphine as catalyst precursors indicate that mononuclear carbonyl−phosphine species are presumably responsible for the catalytic activity.

In the case of heterobimetallic complexes with diphosphines there is a clear difference between the results obtained with the platinum−rhodium and the palladium−rhodium systems. This may be an indication that the active species are not the same as in the case of mononuclear rhodium systems.

High-Pressure $^{31}P\{^1H\}$ and ^1H NMR Studies. To determine the origin of the different catalytic behavior of the heterometallic complexes with diphosphines, we decided to study the dppp systems **1e** and **1h** by HPNMR spectroscopy.

The experiments were performed in two steps: (a) a solution of the complex and excess of the diphosphine was pressurized under 5 bar of H_2 and shaken for 1 h at 50 °C, and the spectra were recorded at different temperatures; (b) the above solution was pressurized with CO up to 10 bar ($CO/H_2 = 1:1$) and shaken for 1 h at 50 °C, and the spectra were recorded at different temperatures.

HPNMR Spectra of 1e/dppp. The $^{31}P\{^1H\}$ NMR spectrum obtained for **1e**/dppp (P/Rh = 4) under 5 bar of H_2 in THF-d_8 (Figure 3a) shows a signal at δ 4.5 ppm with the characteristic satellites ($^1J_{P-Pt} = 2663.6$ Hz), which corresponds to the mononuclear species [Pt(BDT)(dppp)] (**6**).[31] A double triplet at δ 21.2 ppm ($^1J_{P-Rh} = 100$ Hz, $^2J_{P-Rh} = 30$ Hz) and a broad signal at δ 8.2 ppm were assigned to the dihydrido complex $[RhH_2(dppp)_2]^+$ (**7**) by comparison with published data.[25] The signal at δ 3.2 ppm ($^1J_{P-Pt} = 2598$ Hz) along with a doublet at δ 31.3 ppm ($^1J_{P-Rh} = 149$ Hz) may be attributed to the dinuclear species [(dppp)Pt(μ-BDT)Rh(dppp)]$^+$ (**8**). These features are similar to those reported for the related homodinuclear dithiolate rhodium complex $[Rh_2(\mu\text{-BDT})(PPh_3)_2(CO)_2]$[32] ($\delta$ 38.8 ppm (d, $^1J_{P-Rh} = 158$ Hz)), while the P−Pt coupling constant is smaller than that reported for [Pt(BDT)(dppp)],[31] which is consistent with a decrease in the *trans* influence of the dithiolate bridge with respect to the dithiolate chelated in the mononuclear complex.

When carbon monoxide is added to a total pressure of 10 bar (Figure 3b), the signal corresponding to the mononuclear species [Pt(BDT)(dppp)] increases. Two new double triplets at δ 17.8 ppm ($^1J_{P-Rh} = 86.7$ Hz, $^2J_{P-P} = 45.8$ Hz) and δ −9.9 ppm ($^1J_{P-Rh} = 114.7$ Hz) were attributed to $[Rh(CO)(dppp)_2]^+$ (**9**).[25] A new doublet at δ 30.1 ppm ($^1J_{P-Rh} = 116.5$ Hz) in the $^{31}P\{^1H\}$ NMR spectrum together with a double triplet in the hydride region of the ^1H NMR spectrum at δ −9.1 ppm ($^2J_{H-P} = 54$ Hz, $^2J_{H-Rh} = 11$ Hz) are characteristic of the pentacoordinated mononuclear species $[RhH(CO)_2(dppp)]$ (**10**), in which the diphosphine occupies the apical and equatorial position of a trigonal bipyramidal structure.[33] At room temperature there is a fluxional process that interchanges equatorial and apical phosphorus, so the observed coupling constants are an average between both situations. For instance, the related complex $[RhH(CO)_2(bdpp)]$ (bdpp = 2,4-bis(diphenyl)phosphinopentane)) presents a doublet at δ 29.8 ppm ($^1J_{P-Rh} = 112$ Hz) and the hydride signal at δ −8.8 ppm ($^2J_{H-P} = 57$ Hz, $^2J_{H-Rh} = 11$ Hz).[34] For some diphosphines it has been proposed that the $[RhH(CO)_2(diphosphine)]$ species exists as a mixture of the species with the diphosphine in the equatorial−equatorial positions (**ee**) and in the equatorial−apical positions (**ea**).[33]

The variable-temperature $^{31}P\{^1H\}$ NMR spectra confirmed the existence of a fluxional process, since the coupling constant of the doublet signal of **10** changed with the temperature. The different values are 116.5 Hz (rt), 127.4 Hz (−20 °C), 145.1 Hz (−40 °C), and 157.4 (−65 °C). The high value of the P−Rh coupling constant at −65 °C is characteristic of phosphorus in an equatorial position. These data suggest that there may be equilibrium between **ea** and **ee** isomers and it will be displaced to the **ee** species at low temperatures. Unfortunately, the $^{31}P\{^1H\}$ or ^1H NMR spectra could not be further resolved. Small signals at −2 and −4 ppm were not assigned.

The analysis of the spectra of the PtRh complex **1e** with dppp shows that under H_2 pressure some binuclear species are present, but under H_2/CO only the mononuclear rhodium−dppp and Pt−BDT−dppp species are formed (see Scheme 4).

HPNMR Spectra of 1h/dppp. The $^{31}P\{^1H\}$ NMR spectrum of the PdRh **1h**/dppp system under H_2 pressure is more complex than in the case of **1e** (Figure 4a). The double triplet at δ 20.1 ppm and the broad signal at δ 8.0 ppm indicated the presence of the mononuclear rhodium dihydrido species **7**. The singlet at δ 5.8 ppm matches with the value reported for [Pd(BDT)(dppp)] (**11**).[31] Two singlets at δ 12.5 and −0.8 ppm may

(31) Forniés-Cámer, J.; Aaliti, A.; Ruiz, N.; Masdeu-Bultó, A. M.; Claver, C.; Cardin, C. *J. Organomet. Chem.* **1997**, *530*, 199.

(32) Aaliti, A.; Masdeu, A. M.; Ruiz, A.; Claver, C. *J. Organomet. Chem.* **1995**, *489*, 101.

(33) (a) Casey, C. P.; Paulsen, E. L.; Beuttenmueller, E. W.; Proft, B. R.; Petrovich, L. M.; Matter, B. A.; Powell, D. R. *J. Am. Chem. Soc.* **1997**, *119*, 11817. (b) van der Veen, Boele, M. D. K.; Bregman, F. R.; Kamer, P. C. J.; van Leeuwen, P. W. N. M.; Goubitz, K.; Fraanje, J.; Schenk, H.; Bo, C. *J. Am. Chem. Soc.* **1998**, *120*, 11616.

(34) Castellanos-Páez, A.; Castillón, S.; Claver, C.; van Leeuwen, P. W. N. M.; de Lange, W. G. J. *Organometallics* **1998**, *17*, 2523.

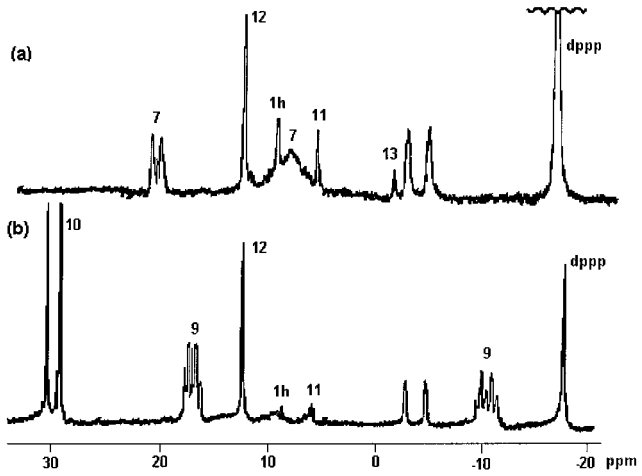

Figure 4. $^{31}P\{^1H\}$ NMR spectrum of **1h**/2dppp in THF: (a) under 5 atm of H_2, (b) under total 10 atm (5 atm of H_2 and 5 atm of CO).

Scheme 4

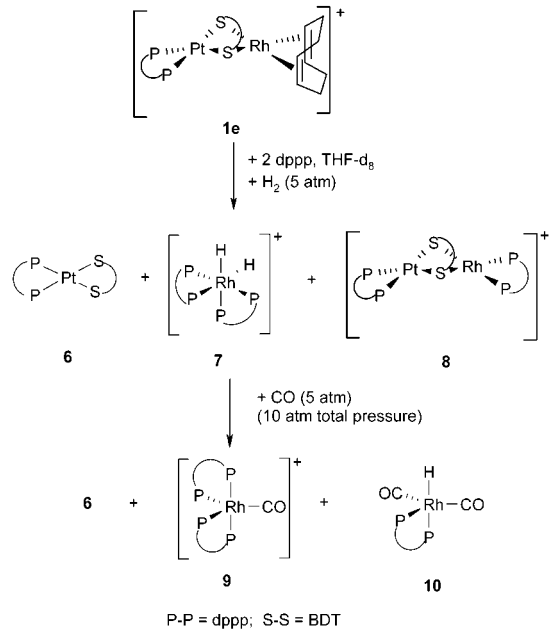

correspond to palladium−dppp species. The signal at δ 12.5 ppm may correspond to a Pd(II) complex, since related Pd(II) complexes such as $[Pd(OAc)_2(dppp)]$, $[Pd(OTf)_2(dppp)]$, and $[Pd(OTf)_2(dppp)]$ were reported to give singlets in the $^{31}P\{^1H\}$ NMR spectrum at δ 11.1,[35] 11.6,[36] and 12.9 ppm,[37] respectively. More deshielded signals have been reported for the ditosilate $[Pd(OTs)_2(dppp)]$ (δ 17.5 ppm in $CD_3C(O)CD_3$)[35] and for the cationic bis(diphosphine) complex $[Pd(dppp)_2](OTs)_2$.[38] So, the signal at 12.5 could be attributed to $[Pd(S)_2(dppp)]^{2+}$ (**12**) (S = solvent). The singlet at δ −0.8 ppm may be attributed to a Pd(0) species (**13**). For instance, the ^{31}P chemical shift reported for the Pd(0) complex

Scheme 5

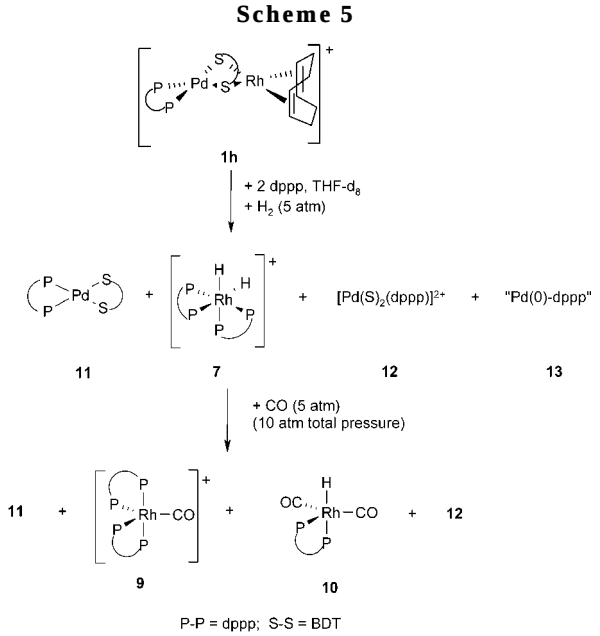

$[Pd(dppp)_2]$ is δ 3.95 ppm in tetrahydrofuran.[39] It has been reported that Pd(0) species form from Pd(II) species through phosphine oxidation.[39] The unreacted binuclear complex **1h** and signals at −2 and −4 ppm were also observed.

Carbon monoxide was introduced to the above solution up to 10 atm CO/H_2; the solution was shaken for 1 h at 50 °C and cooled at room temperature to record the spectra. At room temperature, the $^{31}P\{^1H\}$ NMR spectrum (Figure 4b) shows the signals corresponding to the rhodium monocarbonyl species **9**, the pentacoordinated hydride **10**, the palladium dithiolate **11**, and the palladium(II) diphosphines **12**. Free dppp and the signals at −2 and −4 ppm were also observed. The species formed for this system are summarized in Scheme 5.

To sum up, the above HPNMR spectroscopic data indicated that the PtRh **1e**/dppp and PdRh **1h**/dppp heterobimetallic systems split under catalytic hydroformylation conditions into identical mononuclear rhodium species and the corresponding platinum or palladium fragments. Since the platinum and palladium species are not active in the hydroformylation reaction, the activity of the heterobimetallic systems is due to the hydride rhodium complex **10**. The differences in the catalytic behavior of these two systems can only be explained by the differences in the formation of **10**. Since several equilibria act to form the different species, the concentration of active complex **10** will depend on the stability of the precursor complex. Therefore, the concentrations of complex **10** will determine the activity. In both cases, there was evidence of dinuclear species under H_2, but under CO/H_2 only mononuclear species were detected by $^{31}P\{^1H\}$ NMR.

Concerning the regioselectivity, similar behavior was reported for related thiolate bridging complexes $[Rh(\mu\text{-}S(CH_2)_2NMe_2)(cod)]_2/PPh_3$.[40] The HPIR experiments for this system showed that the species **10** was present,[30]

(35) Drent. E.; van Broekhoven, J. A. M.; Doyle, M. J. *J. Organomet. Chem.* **1991**, *417*, 235.
(36) Makhaev, V. D.; Shul'ga, Y. M.; Dzhabieva, Z. M.; Belov, G. P.; Chernushevich, I. V.; Kozlovskii, V. I.; Donodov, A. F. *Russ. J. Coord. Chem.* **1994**, *20*, 360.
(37) Sanger, A. R. *J. Chem. Soc., Dalton Trans.* **1977**, 1971.
(38) Benetollo, F.; Bertani, R.; Bombieri, G.; Toniolo, L. *Inorg. Chim. Acta* **1995**, *233*, 5.
(39) Amatore, C.; Broeker, G.; Jutand, A.; Khalil F. *J. Am. Chem. Soc.* **1997**, *119*, 5176.
(40) Balué i Paradís, J. Doctoral Thesis, Universitat Autònoma de Barcelona, 2000.

Downloaded by CARLI CONSORTIUM on June 29, 2009
Published on May 22, 2002 on http://pubs.acs.org | doi: 10.1021/om020042r

but the regioselectivities in the hydroformylation of different substrates were different from those obtained with a mononuclear rhodium complex under identical conditions. Since the P/Rh ratio affects the regioselectivity, the degree of dissociation of the starting thiolate complex will affect the P/Rh ratios and, subsequently, the regioselectivity. In our case, since the rhodium species observed were identical for both precursors **1e** and **1h**, the differences in regioselectivity could also be attributed to the different composition of the catalytic solution.

It should also be taken into account that mononuclear platinum and palladium complexes **6** and **11** may act as metalloligands, which may also interfere in the activity and selectivity of the systems coordinating to the active species when the substrate is present.

Conclusion

The reactivity of heterobimetallic PtRh complexes with dithiolate bridges $[(P-P)Pt(\mu\text{-}S-S)Rh(cod)]ClO_4$ toward carbon monoxide and phosphines produces heterobimetallic structures with no cleavage of the bridges in most cases. CV studies showed irreversible oxidation processes, but the species formed could not be identified. Heterobimetallic diene complexes were used as catalyst precursors for the hydroformylation of styrene. The comparison of selectivity data for different catalyst precursors gives no conclusive evidence of the active species, but spectroscopic studies under pressure conditions provide further information. Thus, HPNMR experiments show that mononuclear species are formed under pressure conditions, and therefore, the catalytic activity can be attributed to these mononuclear rhodium species.

Acknowledgment. We thank Ministerio de Educación y Cultura (PB97-0407-C05-01 and PB98-0641) for financial support.

Supporting Information Available: Crystal data and structure refinement, atom coordinates, complete list of bond lengths and angles, anisotropic displacement parameters, and hydrogen coordinates for complexes **2a′** and **3a** are available as Supporting Information. This material is available free of charge via the Internet at http://pubs.acs.org.

OM020042R

Downloaded by CARLI CONSORTIUM on June 29, 2009
Published on May 22, 2002 on http://pubs.acs.org | doi: 10.1021/om020042r